Overview of Physics Research on the TCV Tokamak

A.Fasoli for the TCV Team[1]

Ecole Polytechnique Fédérale de Lausanne (EPFL), Centre de Recherches en Physique des Plasmas, Association EURATOM-Confédération Suisse, CH-1015 Lausanne, Switzerland

E-mail address of main author: ambrogio.fasoli@epfl.ch

Abstract: The TCV tokamak is equipped with high-power (4.5MW), real-time-controllable EC systems and flexible shaping, and plays an important role in fusion research by broadening the parameter range of reactor relevant regimes, by investigating tokamak physics questions and by developing new control tools. Steady-state discharges are achieved, in which the current is entirely self-generated through the bootstrap mechanism, a fundamental ingredient for ITER steady-state operation. The discharge remains quiescent over several current redistribution times, demonstrating that a self-consistent, "bootstrap-aligned" equilibrium state is possible. Electron ITB regimes sustained by EC current drive have also been explored. MHD activity is shown to be crucial in scenarios characterised by large and slow oscillations in plasma confinement, which in turn can be modified by small Ohmic current perturbations altering the barrier strength. In studies of the relation between anomalous transport and plasma shape, the observed dependences of the electron thermal diffusivity on triangularity (direct) and collisionality (inverse) are qualitatively reproduced by nonlinear gyro-kinetic simulations and shown to be governed by TEM turbulence. Parallel SOL flows are studied for their importance for material migration. Flow profiles are measured using a reciprocating Mach probe by changing from lower to upper single null diverted equilibria and shifting the plasmas vertically. The dominant, field-direction-dependent Pfirsch-Schlüter component is found to be in good agreement with theoretical predictions. A field-direction-independent component is identified and is consistent with flows generated by transient over-pressure due to ballooning-like interchange turbulence. Initial high-resolution infrared images confirm that ELMs have a filamentary structure, while fast, localised radiation measurements reveal that ELM activity first appears in the X-point region. Real-time control techniques are currently being applied to EC multiple independent power supplies and beam launchers, e.g. to control the plasma current in fully non-inductive conditions, and the plasma elongation through current broadening by far-off-axis heating at constant shaping field.

1. Introduction

The international research effort in magnetic fusion follows two general, complementary approaches. On one hand, it is crucial to confirm the ITER physics and technology basis by combining elements of tokamak plasma physics that are now independently known into so-called integrated plasma scenarios. On the other hand, more basic studies are necessary to prepare for a fruitful ITER scientific programme and in view of an optimisation of the tokamak concept for longer term developments towards the DEMO stage and commercial reactors. For this, the community needs to address questions that limit our understanding of magnetically confined plasmas and our ability to control them in reactor relevant scenarios, and to explore avenues for improving the plasma performance that may not necessarily be

---

[1] S.Alberti, P.Amorim (IST Lisbon, P), C.Angioni (IPP Garching, D), Y.Andrèbe, E.Asp, R.Behn, A.Bencze (KFKI, Budapest, H), J.Berrino, P.Blanchard, A.Bortolon, S.Brunner, Y.Camenen (Warwick Univ., UK), S.Coda, L.Curchod, K.DeMeijere, E.Droz, B.P.Duval, E.Fable, D.Fasel, A.Fasoli, F.Felici, I.Furno, E.O.Garcia (Risö National Lab., DK), G.Giruzzi (CEA, Cadarache, F), S.Gnesin, T.Goodman, J.Graves, A.Gudozhnik, B.Gulejova, M.Henderson, J.-Ph.Hogge, J.Horacek (IPP Praha, CZ), P.-F.Isoz, B.Joye, A.Karpushov, S.-H.Kim, J.B.Lister, X.Llobet, T.Madeira (IST Lisbon, P), A.Marinoni, J.Marki, Y.Martin, M.Maslov, S.Medvedev (RRC Kurchatov, RF), J.-M.Moret, J.Paley, I.Pavlov, A.Perez, V.Piffl (IPP Praha, CZ), F.Piras, R.A.Pitts, A.Pitzschke, A.Pochelon, L. Porte, H.Reimerdes (GA San Diego, US), J.Rossel, O.Sauter, A.Scarabosio (IPP Garching, D), C.Schlatter, A.Sushkov (RRC Kurchatov, RF), D.Testa, G.Tonetti, D.Tskhakaya (ÖAW, Innsbruck, Austria), M.Q.Tran, F.Turco (CEA, Cadarache, F), G.Turri, R.Tye, V.Udintsev, G.Véres (KFKI, Budapest, H), H.Weisen, A.Zhuchkova, C.Zucca.

addressed by an integrated experiment such as ITER [2]. This latter approach characterises the scientific programme of the *Tokamak à Configuration Variable*, TCV [1]. The TCV facility has been developed to incorporate multiple, uniquely specialized capabilities, in particular high-power (4.5MW), real-time-controllable Electron Cyclotron Heating (ECH) [3-4], and flexible plasma shaping. A growing complement of diagnostics, analysis and modelling tools has led to significant new results in a variety of areas in the period 2006-2008, in spite of a rather short 2007 campaign with no third-harmonic ECRH, followed by a year long shutdown to install several additional diagnostics and new plasma control hardware. This overview illustrates examples of the progress achieved in this period through an extensive use of TCV shaping and EC tools, divided into six main research themes: Section 2 discusses evidence for discharges that are fully sustained in steady-state by the bootstrap current [5]; Section 3 focuses on the observation, interpretation and control of slow plasma oscillations in the presence of internal transport barriers [6]. The effect of plasma shape on stability and transport is discussed in Section 4 [7]; Section 5 summarises the edge physics studies on TCV, presently concentrated on flows in the Scrape-Off-Layer and their implication for transport [8]; Section 6 describes recent developments in real-time control of ECH and EC current drive (ECCD) [9]. Upgrades to the TCV installation are planned with the twofold goal of completing the spectrum of tokamak physics problems that can be addressed and enhancing the reactor relevance of the results, as discussed in Section 7, which concludes the paper.

2. Fully bootstrap sustained discharges for steady-state tokamak operation

One of the modes of operation being considered for ITER steady-state discharges, the so-called advanced tokamak scenario, relies on the attainment of a high non-inductive plasma current component, and in particular a high internally-generated bootstrap current fraction. As strong pressure gradients are needed to drive large bootstrap currents, advanced tokamak scenarios are characterized by internal transport barriers (ITBs). An internal feedback loop governs the current profile, which strongly affects the confinement and thus the properties of the high-gradient region, where in turn the bootstrap current component is localized [10]. As the bootstrap current fraction approaches 100%, external control of the current profile ceases and a total self-consistency of this feedback loop becomes necessary. This requires an exact alignment of the bootstrap current profile with the high-gradient region it engenders. This must additionally be a stable equilibrium point of the internal bootstrap feedback loop: an outward displacement of the current density peak must cause the point of steepest pressure gradient to lag on the inboard side, and vice versa. Whether this is possible depends on the physics mechanisms governing the relation between current and transport. Recent work on TCV has succeeded in answering this question affirmatively. We have produced discharges in which the current is entirely self-generated by the plasma in conditions of intense ECH [11]. This is the culmination of several years of research on electron ITBs, during which the bootstrap current fraction was progressively increased up to 100% [10].

Two different methods were employed to achieve this result. In one scenario, high-power, second-harmonic EC waves are launched perpendicularly to the magnetic field, thus providing no current drive, during the initial plasma current ramp-up. Strong eITBs, with confinement improvement up to a factor of six over L-mode, are generated by the transient negative central magnetic shear that develops in the current penetration phase. The Ohmic flux swing is zeroed immediately after the initial breakdown, cutting off the external plasma current source. Under appropriate conditions, the plasma then evolves spontaneously towards a stationary quiescent state, a stability point of the internal bootstrap feedback loop (Fig. 1). The evolution towards this state is characterized by a shrinking of the region encompassed by the barrier and a reduction of the confinement enhancement down to ~2.5–3.

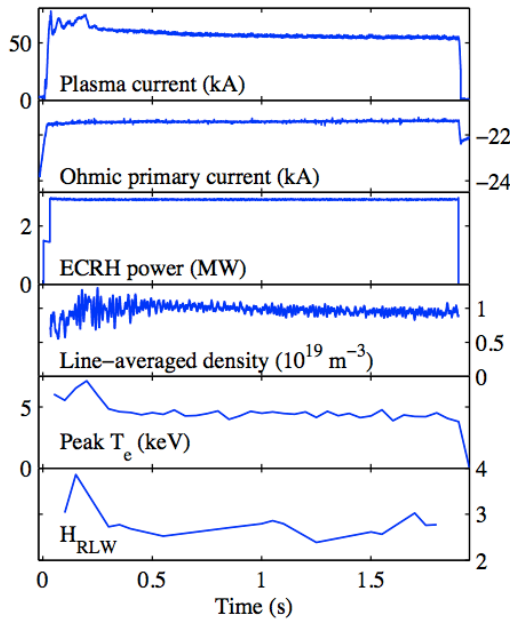FIG.1 TCV discharge 34428. There are no external current sources from 0.02s to 1.9s. A stable current of 55kA (± 2%) is supplied by the bootstrap mechanism from 0.9s to 1.9s. The confinement enhancement factor in the bottom box is normalised to the TCV L-mode scaling.

The normalized temperature profile in the final stable state is shown in Fig. 2, in comparison with a standard Ohmic profile and a standard TCV eITB profile (the latter is from the second experimental scenario described below). Permitting the system to reach this state requires careful tuning of the timing of both the external coil currents and the EC power sources, to minimize the impact of MHD modes that inevitably occur during the initial phase and can either quench the barrier too rapidly or terminate the discharge altogether. Once the stable state is reached, the discharge remains stationary over the time scale of a TCV pulse (1-2s), which is significantly longer than a typical resistive current redistribution time (~150-300ms) and two orders of magnitude longer than the confinement time (~3-6ms). Examples include a 55kA discharge sustained for 1s by 2.7MW heating (see Fig. 1) and a 35kA discharge sustained for 0.6s by 1.35MW heating, both at a line-averaged density of ~10^{19}m^{-3}.
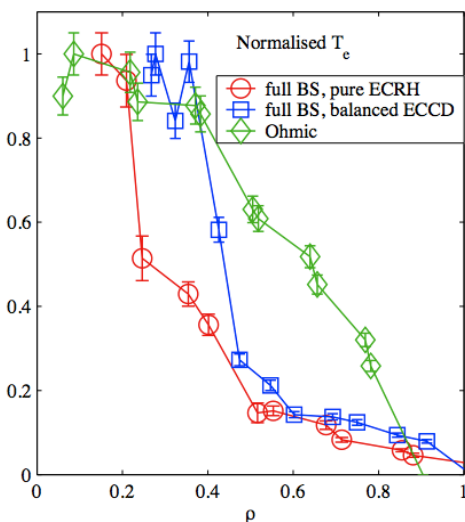

FIG.2 Normalised electron temperature profiles for TCV discharges 34428 (narrow eITB with no ECCD and 100% bootstrap; red), 34175 (broad eITB with balanced co- and counter-ECCD and 100% bootstrap, blue) and 33476 (Ohmic, green). The maximum temperatures for the three cases are 4.3keV, 5.4keV and 0.8keV, respectively.

Following a different approach, we have also succeeded in achieving a 100% bootstrap fraction by annulling the total EC-driven current in pre-existing stationary conditions. Standard stationary non-inductive eITBs [10] are first generated by off-axis co-ECCD; counter-ECCD is then added gradually until the driven current density is nominally zero everywhere. In some cases a quasi-stationary state is indeed established. In this case the region within the barrier remains broad (Fig. 2), with a confinement enhancement factor

around 4-5. As a result, the discharge is not truly quiescent, because of significant MHD activity that cause oscillations and jumps both in the confinement and in the total current. If the spatial profiles of the co- and counter-ECCD distributions are exactly matched, this latter configuration differs from the former only by having a much broader power deposition profile and a sizeable supra-thermal electron population.

3. Slow global plasma oscillations and transport in the presence of eITBs

In TCV, global plasma oscillations affecting several plasma parameters, including the total current and the line-averaged density, are observed in fully non-inductively driven plasmas featuring eITB with strong ECH/ECCD (Fig. 3) [12]. It has been demonstrated that these oscillations are linked to the destabilization and stabilization of MHD modes near the foot of the eITB [13]. Here large pressure gradients are present in a region of low magnetic shear; as a consequence, the ideal MHD stability limit is more easily reached, i.e. infernal modes can become unstable at a lower normalised β value than in standard scenarios. Depending on the proximity to the ideal limit, small crashes or resistive modes can be destabilized, which affect the time evolution of the discharge. Being near marginal stability, the modes can be stabilized by slight modifications of the local pressure and safety factor (q) profiles. If this is the case, the plasma confinement recovers, the shear reverses and the internal transport barrier builds up, until a new MHD mode is destabilized again.
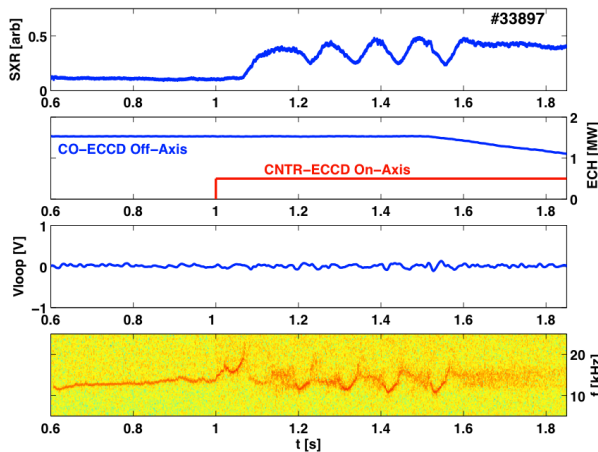

FIG.3 Evolution of line-integrated soft x-ray signal, EC power in the off-axis and on-axis beams, V_{loop} and MHD spectrogram in a fully non-inductive discharge with global plasma oscillations in TCV. At 1.5s, the off-axis power is reduced which changes the q profile, stabilizing the low frequency mode and resulting in a non-oscillating high performance eITB.

A hollow current density profile and the proximity to the infernal mode ideal limit are inherent to these steady-state scenarios, which makes it is very likely that such oscillations will occur in ITER, leading to the loss of a transport barrier and to a confinement degradation. This is why it is important to develop a current density perturbation technique using various actuators that mitigate the deleterious effects of MHD activity.

TCV results show that this cyclical behaviour can indeed be controlled by modifying the current density or pressure profiles, either with Ohmic current density perturbations [12-13] or by modifying the ECH/ECCD power [14]. Figure 3 provides an example of the latter, showing the time evolution of a discharge fully sustained by 1.35MW off-axis co-ECCD. At t=1s an EC beam of 0.45MW is injected on-axis with a counter-CD component, which triggers an eITB with a strong pressure gradient near the q_{min} region. At 1.2s, and regularly afterwards, a large tearing mode at a frequency ~12kHz is generated, reducing the confinement, as indicated by the reduction in the central soft x-ray (SXR) emission (Fig. 3, top trace). The q and pressure profiles are modified by the magnetic island and the mode is stabilized; the barrier forms again until the instability boundary is reached and the mode is once more driven unstable, restarting the cycle. At t=1.5s, the off-axis co-ECCD power is reduced progressively, which changes the q profile. After 1.6s, the profiles are such that the

low frequency tearing mode is stable and the discharge performance remains high, as seen from the SXR trace, despite a lower total EC power injected.

Simulations of steady-state eITBs and of the formation of the electron transport barrier have demonstrated that the confinement improvement is directly linked to the local magnetic shear becoming more and more negative [15]. The study of the particle transport properties of eITBs in TCV has shown that linear gyro-kinetic theory can explain why a dominant thermo-diffusive pinch is observed and leads to very peaked density profiles [16]. For the latter studies a new method to obtain particle pinch contributions from linear gyro-kinetic simulations was developed. Using this method, it has been shown that the collisionality dependence of density peaking in monotonic q profile discharges can also be qualitatively explained. The peaking is maximum near the transition of ITG to TEM turbulence [16].

4. Effects of extreme shaping on MHD stability and transport

Tokamak operational parameters can be extended in TCV by virtue of its flexible shaping capabilities. This permits investigations of discharge optimization and provides a platform to test theoretical models of plasma behaviour [7].
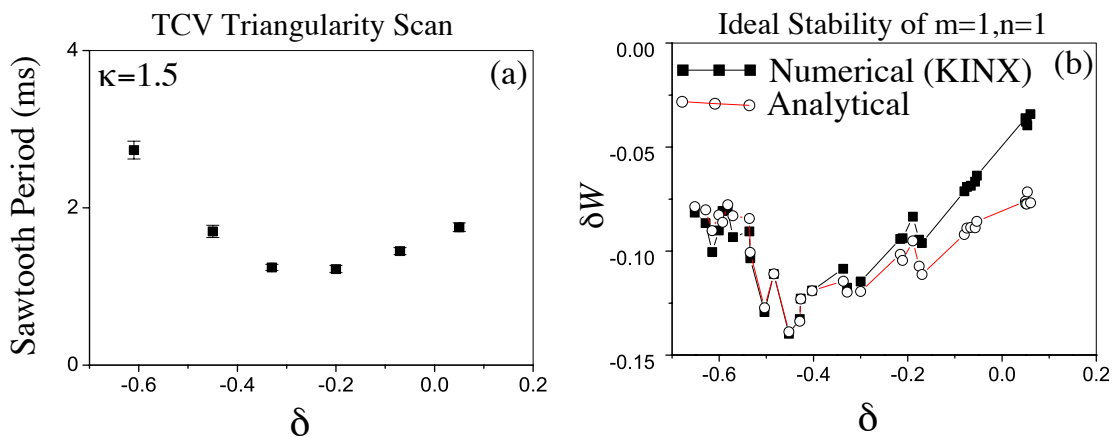

FIG. 4 (a) The measured sawtooth period in TCV, and (b) the potential energy of ideal MHD internal kink mode as a function of triangularity [15].

Plasmas with negative triangularity feature improved MHD stability and transport properties. Both are affected by changes in curvature and gradients of the magnetic field. This was demonstrated explicitly for sawteeth in TCV [17], as shown in Fig 4, since a minimum in the sawtooth period occurs for moderate negative triangularity, roughly coinciding with a minimum in the potential energy of the internal kink mode. This is calculated both numerically and analytically, accounting in both cases for the contributions of the modified toroidal and poloidal curvature due to triangularity.

It should be pointed out, however, that in the experimental triangularity scan described above the elongation at the q=1 rational surface also changes. This small variation can affect the internal kink mode at least as strongly as the triangularity, as proven by the sensitivity of sawteeth to elongation, illustrated by the elongation scan at conventional triangularity shown in Fig. 5 (left). During the elongation ramp, the q profile becomes increasingly broad, with a central value close to unity, such that the n=m=1 mode eventually becomes quasi-stable and oscillates continuously, preventing any peaking in the pressure and the current density profiles [18]. Moreover, under such conditions, the mode structure assumes characteristics of quasi-interchange, namely a q=1 infernal mode, such that several higher harmonics (with m/n=1) are simultaneously destabilised, as shown in Fig. 5 (right). Infernal modes are also seen in TCV when the shear vanishes close to the q=2 or q=3 surface, as discussed in Section 3 on global oscillations in eITB scenarios.
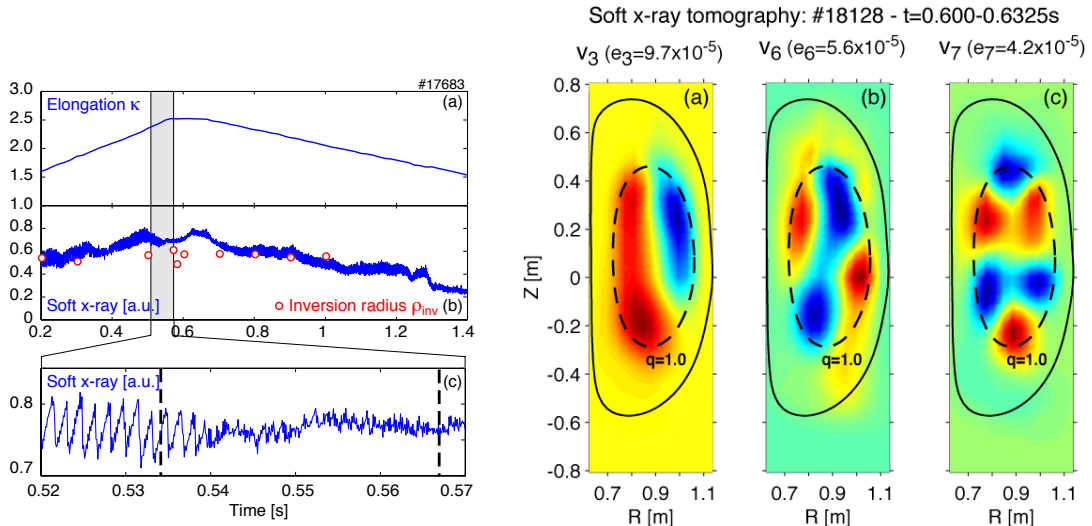
FIG. 5 Left: Evolution of sawteeth during an elongation ramp. Right: m/n=1/1 (a), 2/2 (b), 3/3 (c) components of soft x-ray emissivity during a non-sawtoothing phase of the discharge.

Negative triangularity is also observed to improve the TCV plasma transport properties. A factor of two reduction in the electron heat diffusivity is achieved when going from positive (δ=+0.4) to negative (δ=-0.4) triangularity (Fig. 6(a)) [19]. Extensive gyro-kinetic simulations have been performed [20] to model these experimental conditions. Both in the linear and non-linear phases, negative triangularity is found to have a stabilizing influence on the Trapped Electron Mode (TEM), which in these scenarios is identified as the dominant instability, by modifying the toroidal precessional drift of trapped electrons that resonantly drive the modes.
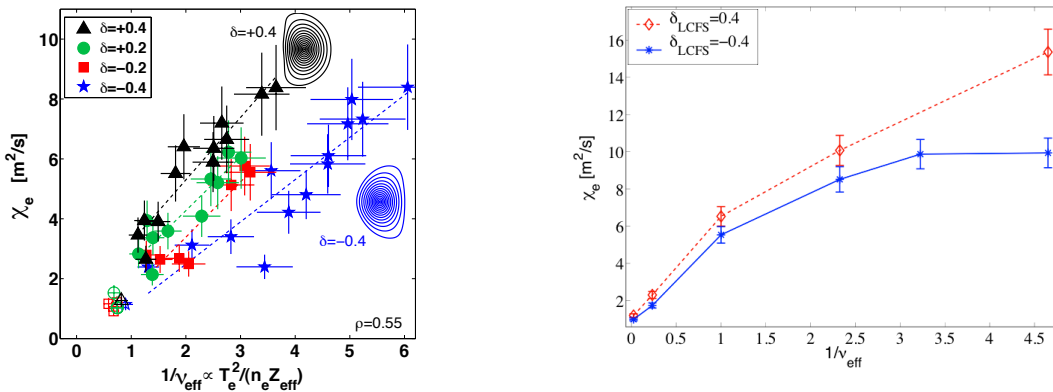

FIG. 6 (a) Experimental electron heat diffusivity at mid-radius as a function of plasma effective collisionality at four different values of plasma triangularity. Full symbols refer to EC-heated L-mode plasmas, while open symbols indicate ohmic plasmas, in which electron transport seems unaffected by plasma triangularity; (b) Effect of collisionality on the electron heat diffusivity estimated from nonlinear simulations based on the GS2 gyro-kinetic code for δ=±0.4.

Negative triangularity also enhances the local shear, which in turn increases the perpendicular wave number (in the ballooning representation $k_\perp^2 = k_\theta^2(1 + s^2\theta^2)$). The consequent reduction in the electron heat diffusivity suggested by a mixing length estimate ($\chi_e \sim \gamma / k_\perp^2$) is confirmed by nonlinear gyro-kinetic simulations, as shown in Fig. 6(b) for a range of collisionality values. Both experiment and simulation demonstrate the stabilising effect of electron-ion collisions.

5. Scrape-Off-Layer transport

The study of Scrape-Off Layer (SOL) transport, both steady state and transient, is a key element of the edge physics research programme on TCV. Recent efforts have concentrated on the study of parallel SOL flow, cross-field turbulence driven particle transport, the link between parallel and cross-field transport and the physics of ELM transport.

Radial profiles of parallel SOL ion flows have been measured in both lower and upper single-null (SNL and SNU) diverted configurations using a reciprocating Mach probe on the machine mid-plane in a series of experiments in which closely matched ohmic density scans are performed for both toroidal field (B_φ) directions (FWD-B and REV-B, where, for FWD-B, the ion $\nabla B \times \mathbf{B}$ drift is directed towards the X-point in SNL). Strong flows are observed at low density ($M_\parallel \sim 0.5$); the flows decrease with increasing density, are co-current directed and reverse direction with B_φ. Remarkably good agreement in both magnitude and direction is found between these measured flows and the neoclassical Pfirsch-Schlüter ion flow estimated on the basis of a large aspect ratio, cylindrical approximation [21]. Taking the mean value of the FWD-B and REV-B flows at any given density reveals a small, yet significant, field independent component when the probe measurement is made either poloidally above or below the mid-plane (Fig. 7). This offset clearly depends on the radial position and density (it increases with density) and is always directed away from the mid-plane. When the same exercise is performed for a magnetic equilibrium such that the probe reciprocates precisely on the plasma mid-plane, the offset disappears at all densities within the measurement error. The fact that roughly the same offset appears above the mid-plane in SNU and below it in SNL (Fig. 7) eliminates the divertor sink as a potential contributor to this offset, while the absence of an offset at the mid-plane is direct evidence for a ballooning type origin of the flow.
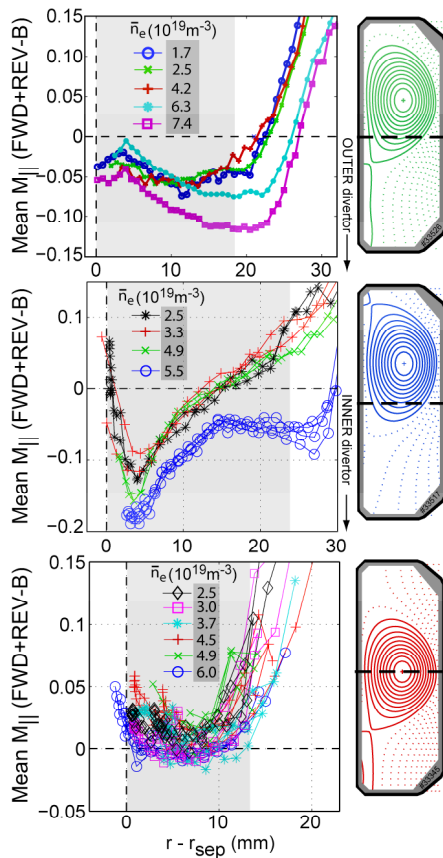

FIG. 7 Mean of FWD and REV-B parallel flows measured on TCV outer mid-plane for ohmic discharge pairs matched in density for three equilibria. The shaded regions delimit the main SOL.

This field independent flow on TCV has been clearly identified with the time average of transient over-pressure generated in field aligned filaments ("blobs") driven by interchange

mechanisms. These structures, identified as high relative fluctuation levels on the Mach probe particle flux time series, increase in number with plasma density, similarly to the observed flow offset behaviour. They are also observed more frequently with decreasing plasma current (at fixed density) and are responsible for the SOL density profile broadening, which is seen either with increasing density or decreasing current. This is consistent with an increase in fluctuations and turbulence driven radial transport as the plasma collisionality increases, and is evidently related to the blob formation process [22].

Filamentary structures are also commonly observed in tokamaks during ELM activity. Direct evidence for this has now been seen on TCV in high time and space resolution IR images of the outer divertor target in ohmic H-modes (Type III ELMs). Field line tracing demonstrates that these filaments are consistent with a release of energy in the outer mid-plane region from a number of discrete toroidal locations, giving mode numbers in the range n ~ 10-20. A filamentary structure is also seen by Langmuir probes in the SOL and at the outboard mid-plane main chamber walls. In the case of Type III ELMs, radial propagation velocities are in the range ~1 kms^{-1} and no acceleration or deceleration is seen in the main SOL within experimental error. On average, between 5-8 substructures are detected at the wall for each ELM (for both Type III and Type I ELMs) and, interestingly, the fluctuating parallel particle flux statistics during the ELM filaments appear very similar to those observed in the inter-ELM phases [23]. A new array of fast radiation detectors based on AXUV diodes has been used to obtain tomographic reconstructions of the radiation distribution during ELMs on a fast (~5 μs) timescale [24]. During Type I ELMs, evolution of radiation in the X-point and inner divertor regions, coincident with the start of Mirnov coil activity, is clearly seen before any particle flux reaches first wall surfaces. Shortly afterwards bright lobes are seen in the outer mid-plane regions (coincident with the detection of filaments at the wall) and later (on the ion transit timescale along field lines) in the outer target vicinity.

The majority of the ELM energy reaching the targets does so in the separatrix vicinity, both for Type I and Type III [25], similarly to JET observations for Type I ELMs [26]. The linear relationship between ELM rise time at the target, τ_{IR}, and parallel transit time from mid-plane to target, $\tau_{\parallel}$, seen elsewhere [24] is also observed on TCV Type III ELMs, but not for the larger (Type I) ELMs seen in X3 heated H-modes, where $\tau_{IR} \gg \tau_{\parallel}$. Modelling of the ELM parallel transport is progressing, using the 2D edge code package SOLPS5 [27] and the 1D particle-in-cell kinetic code BIT1. The numerical results are being tested both against measurements of particle and heat fluxes at the targets and against each other, in particular to better quantify the consequence of fixing heat and particle flux limiters in fluid simulations.

## 6. Real-time ECH and ECCD control

The existing analogue TCV control system is based on matrix multiplication of signals and a PID controller, and is mainly used to control the currents in the poloidal field coils and the plasma current and density. This system was recently employed to control the plasma current and elongation, using the EC system (power and launcher angle) actuators [28], although limited to linear observers and control algorithms. With the development and integration of new, digital real time control hardware, TCV now has the capability to extend real time control techniques to nonlinear algorithms for its multiple EC actuators, including independent power supplies and launchers, with the aim of demonstrating control techniques for example for sawteeth and NTMs. A multi-digital-signal-processor (DSP) controller has been developed in collaboration with IST-Lisbon to replace the PID controller [29]. This system consists of 9 VME cards, each with 4 DSPs and 4 analogue inputs and outputs. The system has been tested successfully to replace the analogue PID system with an algorithm consisting of digital filters which were equivalent to the transformation from the analogue

PID transfer function into discrete space [9]. The development of advanced plasma control algorithms is now proceeding.

As many tokamaks, TCV is equipped with several multi-chord diagnostics producing multiple analogue signals, such as the soft x-ray diagnostic that has up to 256 measurement chords. The present system is clearly insufficient to generate real time observers based on such large numbers of signals. Many of these multi-channel diagnostics use D-tAcq 196 Compact-PCI acquisition cards [30]. These have 96 channels each and can send real time acquired data to a PC host, which has been used to build a real time control system. Integrating this system with Simulink® development and visualisation leads to a powerful, simple controller which may be directly exploited by TCV users, providing an intuitive way to simulate the controller based upon models of the plasma response.

The EC system constitutes a powerful tool for influencing MHD activity in plasmas as it drives localised current, either by reducing the local resistivity or through direct ECCD. The deposition location is controllable by changing the EC launcher mirror angles. The deposition of each of the 6 independent launchers may be controlled in real time, together with the EC power for each cluster of 3 gyrotrons. Initial experiments involving real time manipulation of these actuators were limited to an analogue linear controller, which was able to feedback control the plasma current, elongation and deposition location [9]. In particular, the plasma current was controlled in fully non-inductive ECCD plasmas using the EC power. The plasma elongation was manipulated by tailoring the current profile in a constant magnetic shaping field using far off-axis ECH/ECCD, controlled using the launcher angle. Tracking of the absorption location was demonstrated by using a controller to follow in real time the absorption at constant minor radius as the plasma elongates.
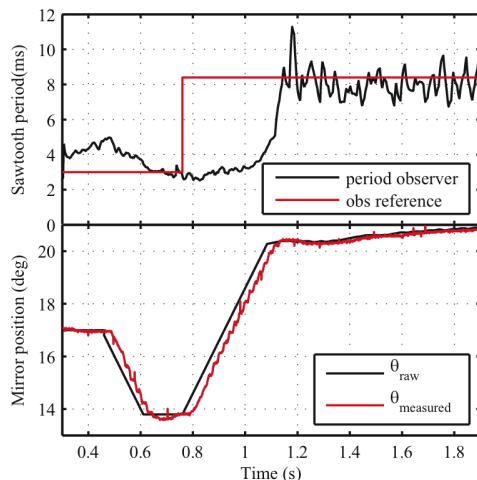
Fig. 8 Sawtooth control using the ECRH launcher angle to control the ECRH deposition around the q=1 surface for shot 35833. Top trace shows the period reference signal together with the measured sawtooth period. Lower trace shows the mirror position.

Experiments to control the sawtooth period were recently accomplished using the D-tAcq real time capabilities. The sawtooth period was changed by modifying the current profile in the vicinity of the q=1 surface. The difficulty with such scheme is that the plasma response is non-linear. Only within a very small angle range does the sawtooth period respond to (small) changes in the launcher orientation, where the controller gain must be low, as opposed to outside this region where the gain should be large. A sawtooth crash detection algorithm was developed for the D-tAcq controller, operating on several core soft x-ray channels. The period was then calculated, averaging over two sawteeth to form the observer. Figure 8 shows the reference and measured sawtooth period signals, as well as the requested and measured mirror position for a first proof of principle. For a more convincing demonstration, the target sawtooth period was not set to a constant value, but to a step function. As the control request increases from 3 to 8ms, the mirror moves to larger angles, which correspond to deposition at smaller minor radii, until the reference is achieved. Such systems are also being developed for

real time equilibrium reconstruction, plasma shape control, real time tomography, profile control, NTM suppression and for triggering diagnostics.

7. Conclusions and outlook: foreseen TCV Upgrades

This paper shows examples of the results obtained on TCV in the last two years, based on an extensive use of its main experimental tools, plasma shaping and ECH/ECCD. Recent evidence for discharges that are fully sustained in steady-state by the bootstrap current is presented, which constitutes a significant step towards the demonstration of the steady-state potential of a tokamak; the physics of eITB regimes characterised by plasma oscillations has been investigated, leading to an identification of the key role played by MHD activity and to ways of suppressing the global plasma oscillations. An unambiguous interpretation of the beneficial effect of negative plasma triangularity on confinement is provided in terms of a lower growth rate and a shorter wavelength of the relevant turbulent modes. The physics of the flows in the SOL was investigated, providing a clear separation between components that are related to neo-classical effects and components that are associated with turbulence and related structures in the SOL. Proof-of-principle experiments on the use of the recently implemented digital control system on TCV were presented, offering great potential for several applications of the real-time ECH/ECCD control.

These results underline the fact that TCV continues to play a complementary role to large integrated tokamak facilities in fusion research, by broadening the physical parameter range of reactor relevant regimes, by exploring fundamental tokamak plasma physics questions and by developing new shapes and control tools. These research lines can be pursued for several more years, in particular taking advantage of diagnostic capabilities that are continuously being enhanced. These include a tangential phase contrast imaging, a reflectometer and a correlation electron cyclotron emission system for the investigation of the physics of turbulence in the plasma core, fast imaging of plasma edge dynamics, a polarimeter for current profile reconstruction, and an improved diagnostic neutral beam and charge exchange system to advance toroidal and poloidal rotation physics [31].

However, in parallel with the start of ITER construction and DEMO studies, TCV may be upgraded to further enhance the spectrum of studies that can be conducted and the reactor relevance of the results. The existing second and third harmonic EC systems provide TCV with momentum-free electron heating and current drive. While these are ITER and, a fortiori, reactor-like features, pure electron heating in the present relatively low density TCV plasmas does not allow for reactor relevant ion heating by equipartition, because confinement times are significantly shorter than electron-ion collision times. Heating at higher plasma densities, together with the implementation of direct ion heating, would vastly augment the attainable T_i/T_e range, filling the entire gap between present, predominantly ion heated tokamaks, and ITER. This would enable validation of models over a wide parameter range, hence stringent tests of our physics understanding and a consolidation of predictions for future devices. On this basis we have investigated potential enhancements in the capabilities of the EC system at the third harmonic and the possible installation of neutral beam injection (NBI) on TCV.

The power of the 3rd harmonic EC system (X3) could be increased by about 3MW (up to 4.5MW), using the present infrastructure, in particular the beam transmission lines and the real-time controllable injectors. With an NBI power of up to 3MW in combination with EC at similar levels, a wide range of the ion to electron temperature ratio could be covered. In the inductive scenario this important parameter could be varied from $T_i/T_e\sim0.1$ to $T_i/T_e\sim2$, depending on the mix of ECH and NBI, naturally covering the typical ITER values ($T_i/T_e\sim1$).

Access for NBI is available through 2 or 3 ports of 15cm diameter allowing near normal injection and possibly a 10cm port for near tangential injection. Most of the power in high density, high current discharges suitable for simultaneous X3 ECH would be provided by

near-normal injection. Target plasmas would include ITER-like H-modes as well as more advanced shapes, which to date have only been studied with Ohmic heating [7]. Their use at the low densities required for simultaneous heating with second harmonic (X2) ECH and ECCD is limited by excessive shine-through losses and high inner wall power loads. At low plasma currents (typically $I_p < \sim 200kA$) orbit losses also become important, although fast ion populations may still be substantial due to the long slowing down times at low density. Injection energies in the range 20-40keV are foreseen, the lowest energies being required to limit losses at low density and current. Injectors would be oriented such that balanced injection is possible, with low enough rotation for studying resistive wall modes.

The proposed NBI system would also provide TCV with an important tool for investigating fast ion and related MHD physics. Tangential access for a 500kW beam would allow for fast ion experiments in plasmas with low density and current, with simultaneous ECH and/or ECCD, i.e. in advanced scenarios, and in the presence of Alfvén wave-particle resonances. Even at these modest power levels, large fast particle populations can be produced, corresponding to a substantial fraction of the Troyon β limit. This would enable experiments directly testing ITER sawtooth control scheme, where localised ECH or ECCD is used to counteract the stabilizing effect of fast ions on sawteeth, with the aim of avoiding large sawtooth crashes susceptible of triggering NTMs.

In conjunction with the NBI fast ion source, the installation of active, low power (50kW) MHD antennas is foreseen, to drive a range of Alfvén modes with high toroidal mode numbers, both for MHD spectroscopy and to perform controlled fast ion redistribution experiments. This would be of interest not only to elucidate aspects of the physics of the transport of fusion α's due to resonant wave-particle interactions, but also as a step towards a possible optimisation of the fusion burn.
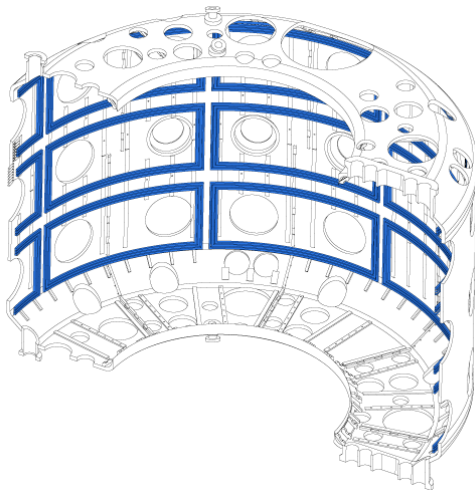
Fig. 9 *Low field side coils for resonant magnetic perturbations (ELM control), fast vertical stabilisation and error field correction.*

An important element for improving the reliability of tokamaks is the control of ELMs and the associated transport and power deposition. The operation of ergodisation coils for ELM control in a variety of plasma shapes and scenarios in TCV would contribute to a basic understanding of the ELM control mechanism, hence to a better assessment of its applicability in ITER and DEMO. With this aim, we are studying the possibility of installing a set of coils for resonant magnetic perturbations (RMP), which would also be employed for correcting error fields. The present concept is based on a coil system at the low-field side (LFS) inner wall, capable of providing simultaneously fast vertical stabilization (by an n=0 component), n=1 error field correction and n=2 or n=4 RMPs for ELM control (Figure 9). For the n=4 design, ELM control would require 4kA-turn (sufficient for island overlap), while vertical stabilisation would be achieved with 5kA-turn, and error field correction with 3kA-turn.

Although establishing a solid predictive capability for fusion performance is paramount, the goal of improving existing performance figures is at least as important. Such improvement is most likely achieved by exploring innovative avenues, such as those allowed by the TCV shaping flexibility. In addition to exploring doublet scenarios and possibly novel divertor configurations [7], the present plan is to equip the low field side of the vessel with power handling tiles for negative triangularity divertors and H-modes, with a potential significant gain in confinement, as demonstrated in L-mode (see Section 4). The proposed package of possible upgrades, conceived and to be implemented in a modular fashion, constitutes an effective way to combine the existing unique TCV features with the needs of advancing the physics understanding, hence our control capabilities, of burning plasmas.

References

[1]   HOFMANN, F. et al., Plasma Phys. Control. Fusion 36 (1994) B277.
[2]   ITER Physics Basis Editors et al., Nucl. Fusion 39 (1999) 2137.
[3]   GOODMAN, T.P. et al., Proc. of 19th Symp. on Fusion Technology, Vol.1, p.565, Lisbon (1996).
[4]   HOGGE, J.P. et al., Nucl. Fusion 49 (2003) 1353.
[5]   CODA, S. et al., EX/2-3, this conference.
[6]   TURRI, G. et al., EX/P3-6, this conference.
[7]   POCHELON, A. et al., EX/P5-15, this conference.
[8]   PITTS, R.A. et al., EX/P4-20, this conference.
[9]   PALEY, J.I. et al., EX/P6-16, this conference.
[10]   GOODMAN, T.P. et al, Plasma Phys. Control. Fusion 47 (2005) B107; CODA, S. et al, Nucl. Fusion 47 (2007) 714.
[11]   S. Coda et al, Proc. 34th EPS Conf. on Control. Fusion and Plasma Phys., Warsaw, Poland, Europhys. Conf. Abstr. 31F (2007) (D-1.008)
[12]   UDINTSEV, V.S. et al., Fusion Sci. Technol. 52, (2007) 161.
[13]   TURRI, G. et al., Plasma Phys. Control. Fusion 50, 065010 (2008); TURRI, G. et al, J. Phys.: Conf. Ser. 123 (2008) 012038.
[14]   UDINTSEV, V.S. et al., accepted for publication on Plasma Phys. Control. Fusion (2008).
[15]   ZUCCA, C. et al, accepted for publication on Plasma Phys. Control. Fusion (2008).
[16]   FABLE, E. et al., accepted for publication on Plasma Phys. Control. Fusion (2008); FABLE, E. et al., to appear in Theory of Fusion Plasmas, Proceedings of the Joint Varenna-Lausanne International Workshop, 2008.
[17]   MARTYNOV, A. et al., Plasma Phys. Control. Fusion 47, (2005) 1743.
[18]   REIMERDES, H., Plasma Phys. Control. Fusion 48, (2006) 1621.
[19]   CAMENEN, Y. et al., Nuc. Fusion 47 (2007), 510.
[20]   MARINONI, A. et al., submitted to Phys. of Plasmas 2008.
[21]   PITTS, R.A. et al., 34th EPS Conf., Warsaw (2007) ECA Vol. 31F, O-4.007 (2007).
[22]   GARCIA, O.E. et al., Plasma Phys. Control. Fusion 49 (2007) B47.
[23]   BENCZE, A. et al., 34th EPS Conf., Warsaw (2007) ECA Vol. 31F, P-2.026 (2007).
[24]   VERES, G. et al., 34th EPS Conf., Warsaw (2007) ECA Vol. 31F, P-2.141 (2007).
[25]   MARKI, J. et al., 34th EPS Conf., Warsaw (2007) ECA Vol. 31F, P-1.053 (2007).
[26]   EICH, T. et al., J. Nucl. Mater. 337 (2005) 669.
[27]   GULEJOVÁ, B. et al., 34th EPS Conf., Warsaw (2007) ECA Vol. 31F, P-1.044 (2007).
[28]   PALEY, J.I. et al., Plasma Phys. Control. Fusion 49 (2007) 1735.
[29]   RODRIGUES, A.P. et al., Fusion Eng. Des. 60 (2003) 435; RODRIGUES, A.P. et al., IEEE Transaction on Nuclear Science 53 (2006) 845.
[30]   http://www.d-tacq.com/acq196cpci.shtml
[31]   DUVAL, B.P. et al., Phy. of Plasmas 15 (2008) 056113.